이학석사학위논문

Discovery of Autophagy Modulator using Image-Based High-Content Screening with Lipid Droplet Bioprobe

지방방울 바이오프로브와 고효율 이미지 기반 스크리닝 시스템을 통한 자가포식 저분자 조절 물질 개발

2015년 8월

서울대학교 대학원

화학부 생화학 전공

유 빈

Abstract

Discovery of Autophagy Modulator using Image-Based High-Content Screening with Lipid Droplet Bioprobe

Bin Yoo

Department of Chemistry, Chemical Biology

The Graduate School

Seoul National University

Autophagy is a major clearance and pro-survival pathway for recycling cytoplasmic components and for the removal of disease-causing aggregated proteins, organelles, and lipid droplets by lysosomal degradation [1]. Basal level of autophagy is essential for balancing the protein quality and degradation and recycling of cellular components while maintaining cell viability. The formation of intra-neuronal mutant protein aggregates is a key characteristic of several human neurodegenerative diseases such as Alzheimer's disease and Amyotrophic lateral sclerosis (ALS). Therefore, protein degradation can enhance the clearance of misfolded and accumulated protein aggregates that have not been efficiently degraded due dysregulated autophagy. This enhancement of aggregated protein clearance may ameliorate neuro-degeneration disease [2]. Herein, we aimed to identify a novel small molecule autophagy modulator using our fluorescent bio-probe Seoul-Flour 44 (SF44) to monitor hydrophobic cellular lipid droplets and lipid metabolism, which can be mediated by the autophagy process. This lipid droplet (LD) screening method was applied to a phenotypic and cell image-based high-content screening (HCS) system in living cells, and it can discriminate the effects of chemical modulators on autophagic flux with cellular LD levels as a late-stage marker of autophagy [3]. As a first step, about 1400 library compounds were screened using SF44 to identify active lead

compounds that can induce autophagy without causing cytotoxicity and off-target effects. The primary positive compounds were further tested by western blot analysis of LC3 lipidation and p62 to monitor autophagy. Then, mechanism of-action study of the hit compound confirmed that it stimulates mTOR-independent autophagy, and the hit compound was further investigated by a structure-activity relationship analysis (SAR) in search of a potent and promisingly active compound structure. We also discussed the possible implications of autophagy inducer in cellular ALS models that the autophagy induction mitigates neurodegeneration by acting directly on mutant SOD1 clearance, which can be potential therapeutic approaches for ALS and related conditions. This study will be informative for the growing field as research tools and developing drugs for autophagy-related diseases such as Alzheimer's and ALS diseases, for which there have been many failures of target-based drug candidates in clinical trials. In-depth characterization of the compound properties including target identification can aid in the design of improved next-generation drugs for neurodegenerative diseases.

Keywords: autophagy, amyotrophic lateral sclerosis (ALS), neurodegenerative diseases, Seoul-Flour 44 (SF44), lipid droplet (LD) screening, high-content screening (HCS), autophagic flux, autophagy modulator, LC3, p62, , mechanism of-action study, mTOR-independent autophagy, structure-activity relationship analysis (SAR), cellular ALS models, mutant SOD1, Alzheimer's disease, target identification

Student Number: 2011-23231

Contents

1. Introduction

Autophagy is an intra-cellular degradation system which degrades a variety of cellular components, including lipids, glycogen, organelles, proteins, and intracellular pathogens within lysosomes in order to maintain cellular homeostasis under both normal and stress conditions [4 and 5]. Specifically, autophagy involves the dynamic rearrangement of subcellular membranes to sequester cytoplasm and organelles and, autophagy marker proteins which direct membrane docking and fusion for delivery to the lysosome are important components of autophagy. In general, the process of autophagy can be distinguished into 4 steps: (1) induction, (2) the formation of double-membrane structures called autophagosomes, (3) which fuse with lysosomes to form autolysosomes, (4) where engulfed cytoplasmic contents are degraded [6]. Conventional autophagy is characterized by the recruitment of lipidated LC3 to autophagosomal membranes and degradation of polyubiquitin-binding protein p62. Endogenous LC3 is processed post-translationally into cytosolic LC3-I, and this LC3-I is converted to LC3-II, which associates with autophagosomemembranes [7]. Another, autophagic flux can be determined by the measurement of p62 because p62 is an adaptor between autophagic machinery and ubiquitinated proteins via ubiquitin-binding and LC3 interacting regions (Image 1) [8]. Consequently, autophagy virtually impacts on cellular function and signaling pathways.

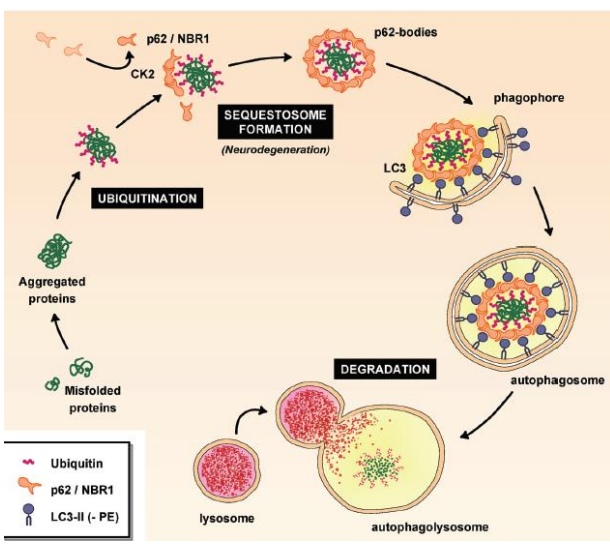

Image 1 Autophay flux. The drawing represents a simplified overview of the factors and processes required in autophagy process

Although aging and genetic mutation have been implicated in the occurrence in human disease states, such as

cancer and neuro-degeneration, defective or aberrant function of autophagy can be the principal risk factor and is intimately associated with development and progression of such human diseases. This highly regulated process is critical for recycling nutrients and removing damaged and aggregated proteins, since several neurodegenerative disease conditions, including amyotrophic lateral sclerosis (ALS), are commonly caused by accumulation of mutant proteins, superoxide dismutase 1(SOD1) in ALS [9]. Previous studies have also suggested that alteration of the autophagic process is involved in neurodegeneration, as affected neurons usually exhibit accumulation of autophagosomes or autolysosomes [10]. In addition, sustained expression of the mutant SOD1 is the result in decreased autophagic activity, and the aggregates formed by these proteins are relevant to toxicity and reducing the levels of these proteins may be beneficial [11]. Thus, these disease-causing aggregation-prone proteins, mutant SOD1 in ALS, could be cleared by autophagy in cultured cell models and mouse models [12 and 13].

A number of small molecule autophagy modulators have been identified from a phenotype based high-throughput screening [14]. The method of the phenotype based HTS allows easy handling and rapid screening of small molecule libraries and has become popular techniques not only to identify novel therapeutic agents, but also to clarify the role of autophagy in neuro-degenerative disease. It has greatly contributed to frame a hypothesis that a certain compound has the ability from a collection to interfere with a biological process or disease model in live cells.

The identification of small compounds that modulates autophagy activity through High-content screening (HCS) is limited by the lack of methods to specifically quantify each step of the autophagy process. In traditional high-throughput drug screens, individual compounds from a small molecule library are used to suppress the enzymatic activity of a target protein [15 and 16]. However, this traditional screening method has been only successful for known target proteins, and the specific enzymes responsible for human disease are mostly unknown. A detection of green fluorescent protein-microtubule-associated protein 1 light chain 3B (GFP-LC3) puncta assay has been widely used in tacking specific autophagy component vesicles, microtublule-

associated protein 1 light chain 3B (LC3B) by tagging green fluorescence protein (GFP-LC3)[17]. The fact that LC3 is known as a component of the autophagosome which diffuses to puncta dots during autophagy, its fluorescent fusion protein can be monitored in the process of selective autophagy. However, LC3-GFP fluorescence is quenched upon fusion between autophagosome and lysosome due to the low lysosomal pH. Therefore, this method for monitoring autolysosome formation and degradation events is restricted to discriminate individual steps of the autophagyic pathway. Given this potential limitation, mCherry-EGFP-LC3 puncta assay has been generated, which overcomes the limitation by utilizing the difference in pH sensitivity between GFP and mCherry in live cells and allows for concurrent monitoring of multiple steps within the autophagic and endolysosomal process [18].

Intriguingly, many of early approved drugs that were discovered using a phenotypic screening and were approved by FDA have an unknown mechanism of action [19]. Even today, compounds that are widely known as autophagy modulators, including chloroquine, resveratrol and rapamycin, none are specific for autophagy and have undesirable off-target effects and cytotoxic effects by modulating other cellular activities [20]. Although the compound activating autophagy via the mammalian target of rapamycin (mTOR) pathway may exert powerful inducing autophagy effects in disease models, but cytotoxic or cytostatic effects cannot be prevented in cancer models [21 and 22]. To rule out the possibility of multiple off-target effect, autophagy studies represent an attractive target for pharmaceutical manipulation, and a robust screen is needed to identify compounds that specifically target the events within the autophagic pathway.

To overcome the disadvantages described above, our lab utilized Seoul-Flour 44 (SF44) as a fluorescent bioprobe not only to monitor autophagy process in living cells via visualization of cellular lipid droplets, but also to identify the impact of compounds on autophagic activity by specifically targeting the events within the autophagic or autolysosomal pathway, as they share many cellular regulatory mechanisms [3]. Autophagy promotes cellular lipid metabolism and releases lipid droplets to lysosomes for degradation of fat stores to free fatty acids, as cellular lipid stores triglycerides in

lipid droplets for energy source [23]. Eventually, cellular lipid droplet metabolism is promoted by induction of autophagy during nutrient deficient condition [24]. Due to the unique hydrophobic environment of LDs, SF44 gets fluorescence specifically inside the LDs. The LD screening platform is successful for HTS and HCS with chemical libraries. A various contents for single cell information, including the size and quantity of cellular LDs, cell morphology, and solubility of compound can be obtained from a single operation [3]. In addition, false-positive hits which are the key problematic in the field of HTS, can be excluded and can be even discriminated from the hit compounds using our HTS approach. Herein, we demonstrate that mTOR-independent autophagy inducer, multiparametric screening outperforms conventional autophagy assays, and we identified a specific enhancer of autophagic flux using HTS approach through a phenotypic and cell image-based assay with lipid droplet bioprobe.

2. Results and Discussion

2.1 Autophagy inducer via SF44-based high content screening (HCS)

In fact, there has been a rapid increase in reports on drug discovery of autophagy, and various small molecule autophagy modulators have emerged in the past few years. Although this has revealed many drugs of potential clinical utility, the tools to measure autophagy are imperfect and require multiple assays to allow robust conclusion to be made about physiological changes. Rapamycin, 3-methyladenine (3-MA), and bafilomycin A1 are the most widely used in autophagy research, but none of them are specific for autophagy and have undesirable off-target and cytotoxic effects by modulating other cellular activities. For example, rapamycin exerts powerful autophagy-inducing effects via mTOR pathway, but it affects a wide range of cellular responses, such as protein synthesis and cellular metabolism. 3-MA is used at very high concentrations to inhibit autophagy (usually 10 mM), but it can target other kinases and affect other cellular processes such as glycogen metabolism. Indeed, its effect is beyond its role in autophagy inhibition. Even though bafilomycin A1 is very useful to assess autophagic flux as an autophagy inhibitor by blocking the fusion between lysosome and autophagosome, it mainly affects lysosomal degradation by inhibiting acidification. In addition to the compounds described above, numerous other compounds have been described that induce autophagy, including resveratrol, spermidine, and BH3 mimetics [1]. Although these compounds can effectively suppress and induce autophagy, the precise mechanisms by which some of these compounds induce autophagy are still unclear, and many of these drugs and their targets affect processes that are distinct from autophagy. Therefore, a more direct evaluation of autophagy-dependent effects remains to be clarified.

Most popular assays for autophagy modulators are GFP-LC3 puncta count as readout for autophagic activity as a primary phenotypic screen, as this correlates with

autophagosome numbers [18] and western blots of LC3 I and LC3 II forms. A common misconception is the notion that increased numbers of autophagosomes in cells correspond to increased cellular autophagic activity. Not only LC3 vesicle count or the number of autophagosomes can increase when autophagy is induced, but it also increases if autophagosome degradation is blocked in the autophagy pathway downstream of autophagsome formation [25]. In many cases, apparently discrepant results can be explained by LC3-based assays because this assay has not accounted for the effects of flux and has easily misinterpreted LC3 vesicle counts or increases in LC3 II as being simply due to increased autophagosome formation. Given these potential limitations, the development of more specific autophagy modulators screening system is vital, which allows the effective discrimination from false-positives and allows direct observation of autophagic flux without any genetic perturbation.

Lipid droplets are particularly prominent in the adipose tissue, where they organize as a single large droplet, but all cells contain lipid droplets to variable extents [26]. When cells need energy or prevents enlarged fat stores, the lipids inside the LD not only gets degraded solely through specific lipid-mediated lipolysis by acidic lipases, but authophagy can also contribute to lipid catabolism [27] for maintain of cellular energetic balance. Our lab focuses on the contribution of autophagy to lipid metabolism by monitoring the lipid droplets with SF44 in living cells without transfection and cytotoxicity. Seoul-Fluor 44 (SF44) is an indolizine-based structure which enables specific and selective staining of hydrophogic LDs, assorting the polar organelle in the cellular system, such as cytoplasm (Fig. 1) [3].

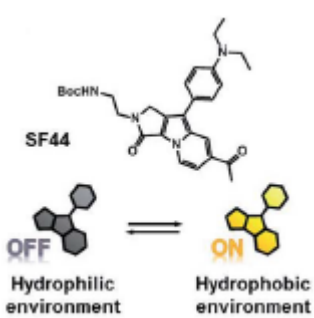

Fig. 1 Chemical structure of SF44 and its fluorogenic features after exposure to a polar environment [3].

It is nontoxic and requires no fixation and washing steps as compared to commercially available fluorescent dye used for the staining of lipids [28]. Therefore, SF44 is perfectly suitable for the targeting LDs and monitoring the

quantity and the size of cellular LDs. Considering LDs are hydrophobic organelle filled with neutral lipids, the specificity of a LD probe, SF44, can be a novel fluorescent turn-on bioprobe to monitor autophagic flux [3].

To establish cell-based auotphagy HTS using SF44, our lab has optimized the fluorescence imaging protocol for identifying autophagy modulators on a 96-well plate in a high-throughput manner [3]. 96 individual wells are captured images after incubation with SF44 and Hoechst for 30min. Those captured images are then analyzed with organelle quantity, size, and fluorescence intensity of LDs. Cell morphology and cytotoxic effect also can be readily checked. With the optimized autophagy HTS, we screened an in-house library constructed using a privileged-substructure-based diversity-oriented synthesis (pDOS) strategy. About 1440 library compounds were screened in HeLa cells in a primary phenotypic screen (Fig. 2).

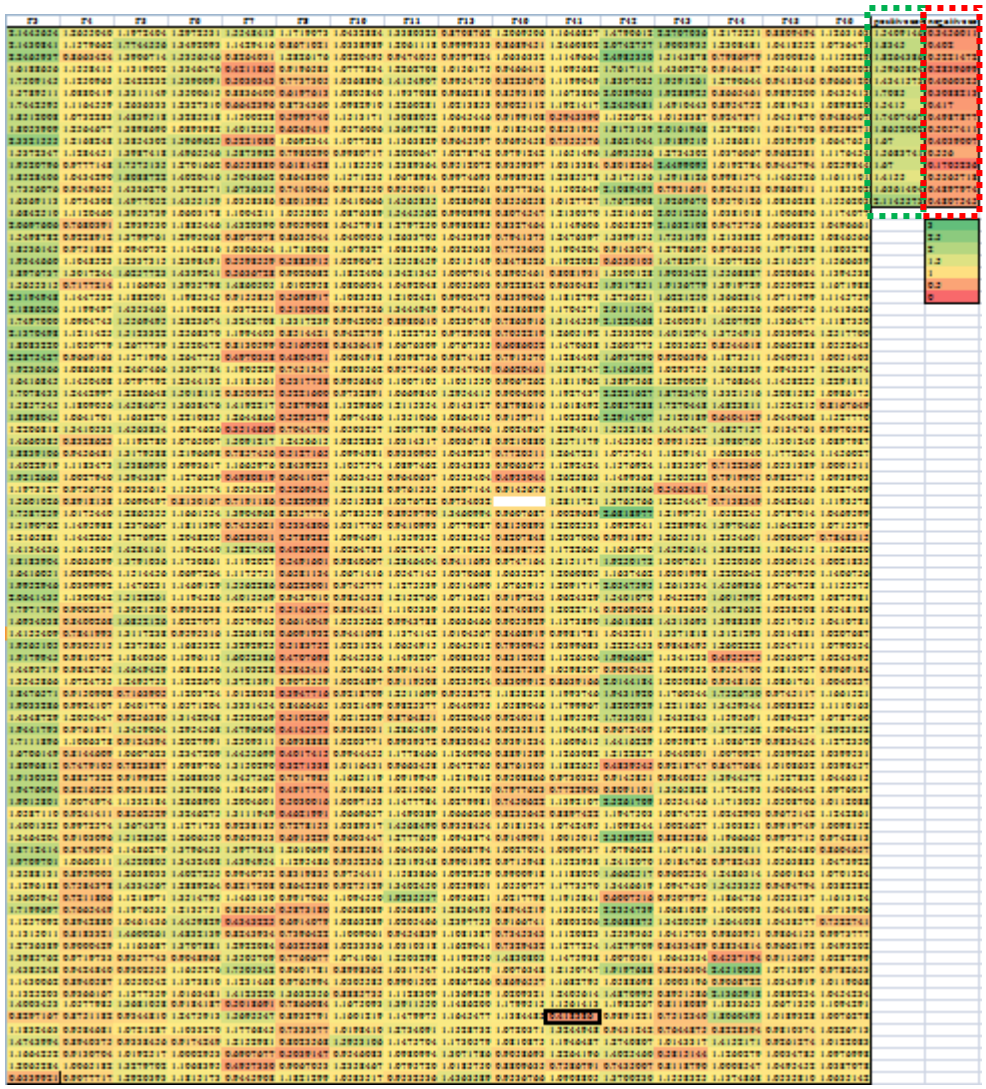

Fig. 2 Hit map of high-content screening (HCS) of small molecule modulators on LDs with SF44. The results analyzed with lipid organelle counting per cell. Green dotted box represents positive control and red dotted box represents negative control.

The results from autophagy HTS screening were analyzed with fitting between organelle counting and total organelle area in order to show linear correlation between the two and to eliminate unwanted positives. Outliers observed data points that were deviated from linearity are due to cell shrinkage, cell division, or aggregation of compounds. And, those potential false positives were excluded from possible hit

compounds [3]. After image-based data analysis, primary hit compound, P41H06, was subjected to secondary screening in a dose-dependent manner (Fig. 3). P41H06 dramatically reduced cellular LDs in a dose-dependent manner with IC_{50} values of 11.52 μM, quantitative measurement of the LD-decreasing potency calculated by organelle counting (Fig. 4).

(a)

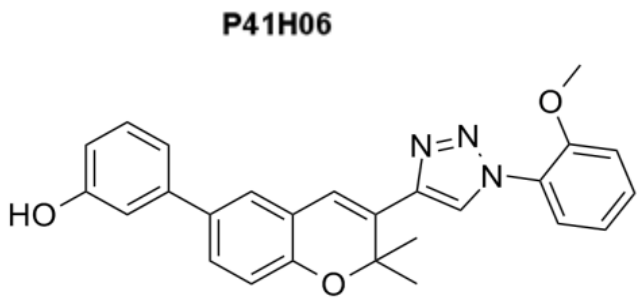

(b) (c) (d)

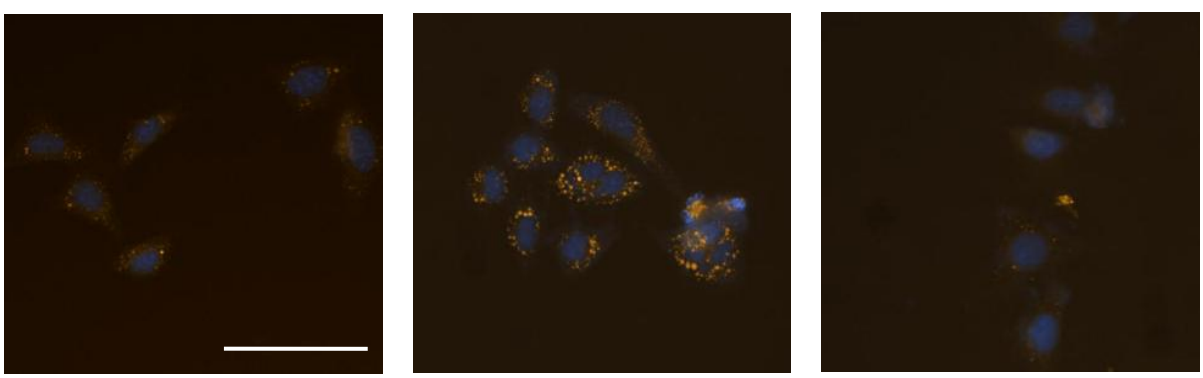

(e) (f) (g)

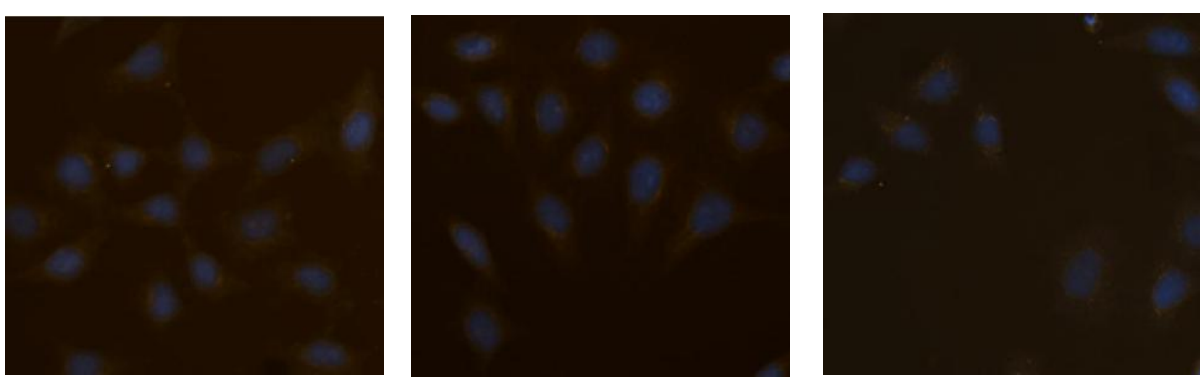

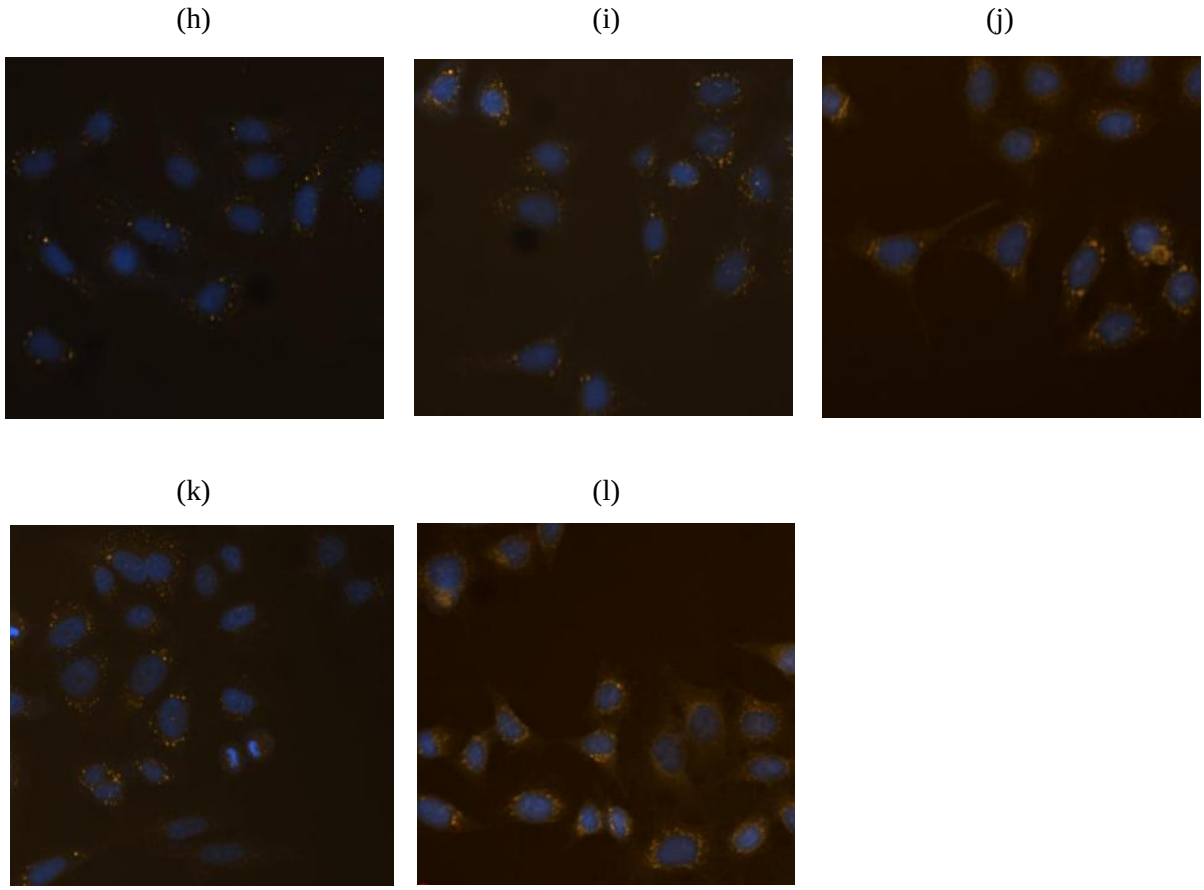

Fig. 3 Representative fluorescence images from In Cell analyzer2000 ((b)~(l)) and chemical structure of P41H06 (a). (b) DMSO as control, (c) Oleic acid as a positive control, and (d) serum-free starvation as a negative control. HeLa cells were treated with the hit compound at various concentrations for 24 h: (e) 40 μM of P41H06, (f) 20 μM of P41H06, (g) 10 μM of P41H06, (h) 5 μM of P41H06, (i) 2.5 μM of P41H06, (j) 1.25 μM of P41H06, (k) 0.625 μM of P41H06, and (l) 0.3125 μM of P41H06. Images were visualized using SF44 (orange) and Hoechst (blue).

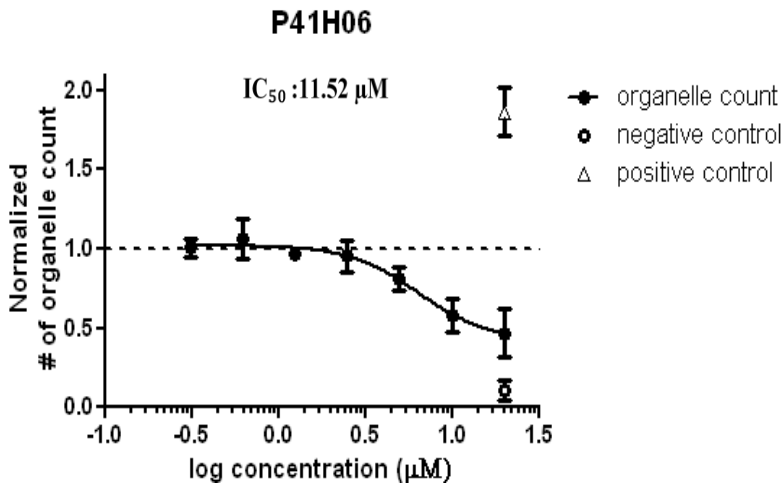

Fig. 4 Dose-dependency curve on cellular LDs analyzed with organelle counting with treatment of P41H06.

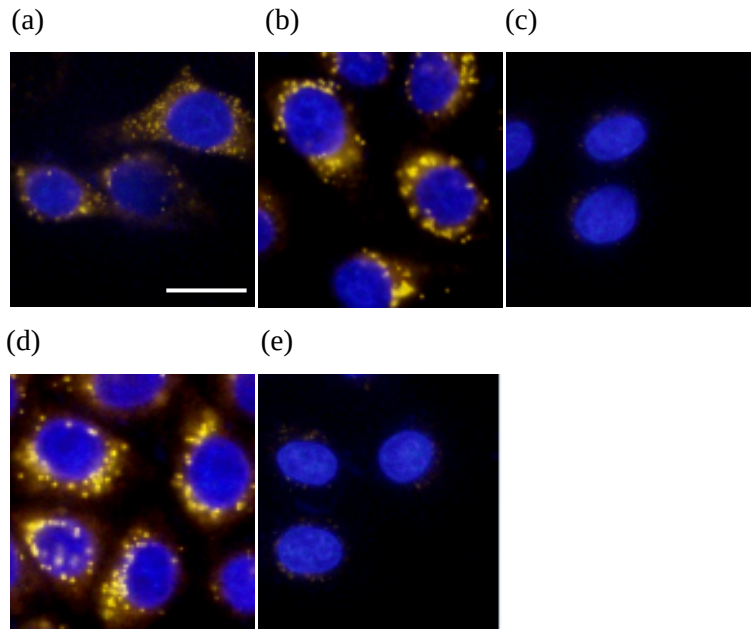

Fig. 5 Representative fluorescence images from Olympus fluorescence microscope, 100X. Autophagy regulation in HeLa cell with known auophagy modulators. Cellular LDs stained with SF44 in HeLa cells under various conditions. Cells were incubated for 6 h with (a) DMSO as control, (b) 5 µM of oleic acid as a positive control, (c) 100 nM of rapamycin to induce autophagy, (d) 10 nM of bafilomycin A1 to inhibit autophagy at a late stage, and (e) 20 µM of P41H06. Fluorescence images were visualized using Hoechst (blue) and SF44 (yellow). The scale bar represents 20 µm.

As proof of concept, we analyzed conventional autophagy regulators, including rapamycin and bafilomycin A1, and revealed striking conditional dependencies of rapamycin and bafilomycin A1 through SF44-based LD visualization. As Fig. 5 shows, a significant reduction in LDs could be visualized by treatment with P41H06 and rapamycin, which suppresses mTOR-dependent inhibition of autophagy. On the other hand, increased cellular LDs was observed with treatment of bafilomycin A1 which inhibits autophagic flux by blocking the fusion between autophagosomes and lysosomes. In addition, oleic acid was used to promote the formation of cellular LDs. These outcomes confirmed that autophagy regulates cellular lipid metabolism, and autophagy was induced notably with gradual increases of cellular LDs after treatment with P41H06.

2.2 P41H06-induced autophagy in HeLa cells

To test if the effects of P41H06 were dependent on autophagy, we did western blot analysis on autophagic regulation with LC3 and p62 was performed. The conversion of endogenous LC3 I to LC3 II reflects autophagosome formation and autophagy activation [29]. And, the measurement of p62 expression strictly serves as an indicator of autophagic flux, and consequently, p62 is degraded following an increase in autophagic flux for which this protein currently serves as an indicator [8]. As shown in Fig. 5(a), nutrient starvation, the most well-known autophagy-inducing condition and P41H06 treatment in HeLa cells resulted in increased LC3 I to LC3 II conversion in a dose-dependent manner. Its conversion was significantly augmented in a dose-dependent manner compared with DMSO treated control cells. Since LC3 II levels relative to β-actin correlate with autophagosome number per cell [30], autophagosome number was quantified (Fig.5(b)). Although an increase in LC3 II by P41H06 was due to increased autophagosome formation, accumulation of LC3 II could also occur if there is impaired autophagosome-lysosome fusion. So, we confirmed our results with the measurement of p62 expression as a marker of autophagic flux. And, impaired autophagic flux was confirmed by lack of decrease in p62 after treatment of autophagy inhibitor, 3MA. Similar results were obtained with the analysis of p62 levels. The

cellular level of p62 was degraded upon serum deprivation and P41H06 treatment, suggestive of induction of autophagy and an increase in autophagic flux. Taken together with the outcome of the LD HTS assay and the quantification of normalized LC3 II and p62 to β-actin (Fig. 4), these data suggest that P41H06 elicits substantial autophagy activation in HeLa cells.

(a)

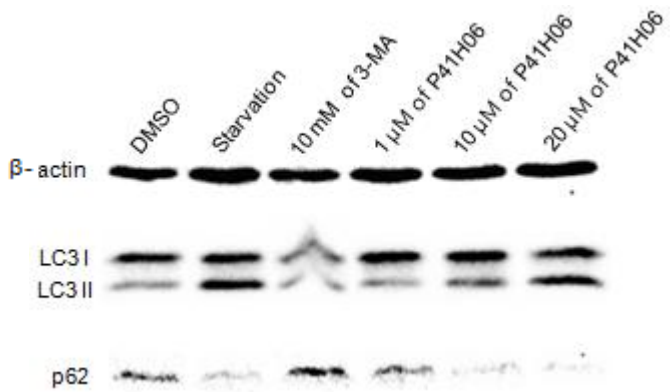

(b)

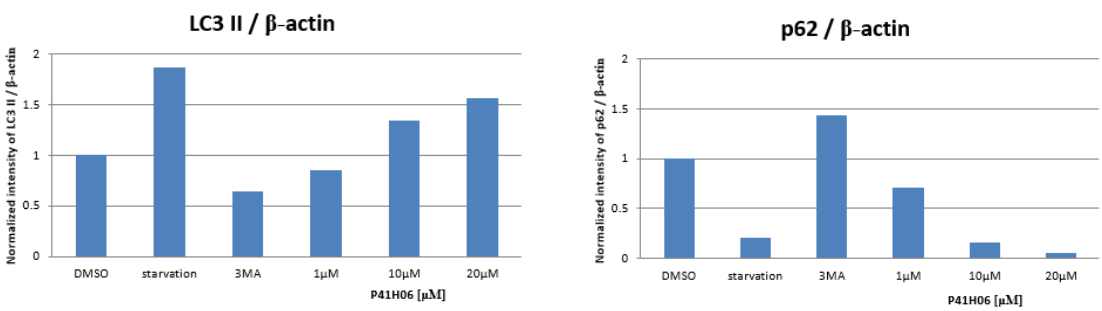

Fig. 6 Western blot analysis on autophagic regulation with LC3 and p62. (a) The proteolytic conversion of LC3 I to LC3 II and the degradation of p62 were monitored via western blot analysis upon treatment with P41H06 at various doses. 10 mM of 3-MA (negative control) and serum starvation (positive control) were also treated in HeLa cells for 6 h. (b) Data in bar graphs represent the lapidated LC3 II and p62, normalized to β-actin.

2.3 Modification of hit compound

In order to examine the structural and functional study of hit compound, new focused compounds were constructed in the effort of optimization of hit compound structure into advanced compounds as an autophagy inducer. New compound structures are based on the structure of hit compound with different functional groups at R_1 position. Table 1 shows the chemical structures that are structurally similar to the hit compound, and the study demonstrated that any changes in the functional group at R_1 position rendered significant different activity on autophagy and even resulted in the complete loss of autophagy-inducing activity of the compounds. The expression of the autopahgic proteins, LC3 and p62, were measured following treatment with compounds (Table 1).

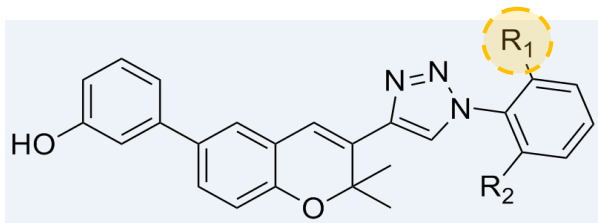

R_1-substituent	**R_2-substituent**
CH3	H
F	H
Ph	H
MeS	H
NH2	H
CN	H
MeO	MeO
MeO	H

Table 1 Modification of hit compound to test autophagy inducing activity.

(a)

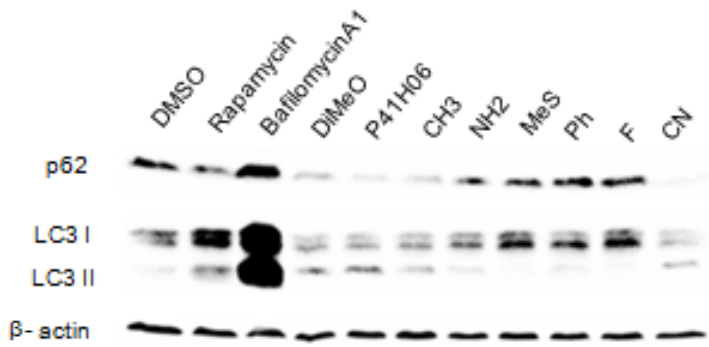

(b)

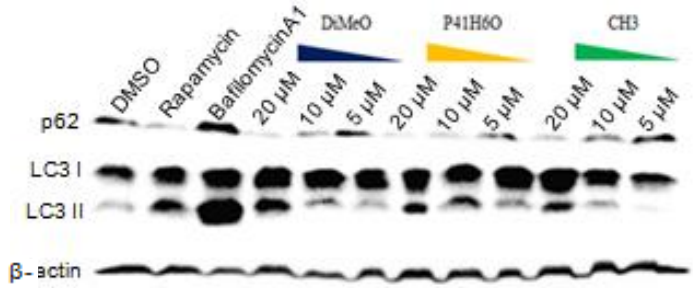

Fig. 7 Effect of compounds on autophagy inducing activity. The proteolytic conversion of LC3 I to LC3 II and the degradation of p62 were monitored via western blot analysis upon treatment with P41H06, DiMeO, and CH3 at various doses. 100 nM of rapamycin (positive control) and 10 nM of bafilomycin A1 (negative control) were also treated in HeLa cells for 6 h. (a) The cells were treated with 100nM Rapamycin, 10 nM Bafilomycin A1, 20 μM of various compounds for 6 h. (b) DiMeO, CH3, and P41H06 induce autophagy in HeLa cells in a dose-dependent manner.

As shown in Fig. 7, the expression of p62 in HeLa cell was diminished by rapamycin, CH3, DiMeO, and P41H06 treatment. The results revealed that the levels of LC3, particularly LC3 II, had increased, leading to an increased ratio of LC3 II / LC3 I in a dose-dependent manner following rapamycin, CH3, DiMeO, and P41H06 treatment.

These results suggested that CH3, DiMeO, and P41H06 induced autophagy by regulating p62 and LC3 II, but DiMeO and CH3 functional groups showed less potency of autophagy inducing effect than that of lead compound with no or minimal cytotoxicty. In addition, it can be seen that a notable diminished autophagy inducing activities and even toxicity were observed when the MeO functional group was replaced by electron withdrawing groups such as F and CN (Fig. 8). These results further supported our postulation that methoxy group at R_1 position might play a significant role in the biological activity. The structure of hit compound acting on autopahgy gave us new insights into the structural and functional relationship of this class of compounds as autophagy inducer.

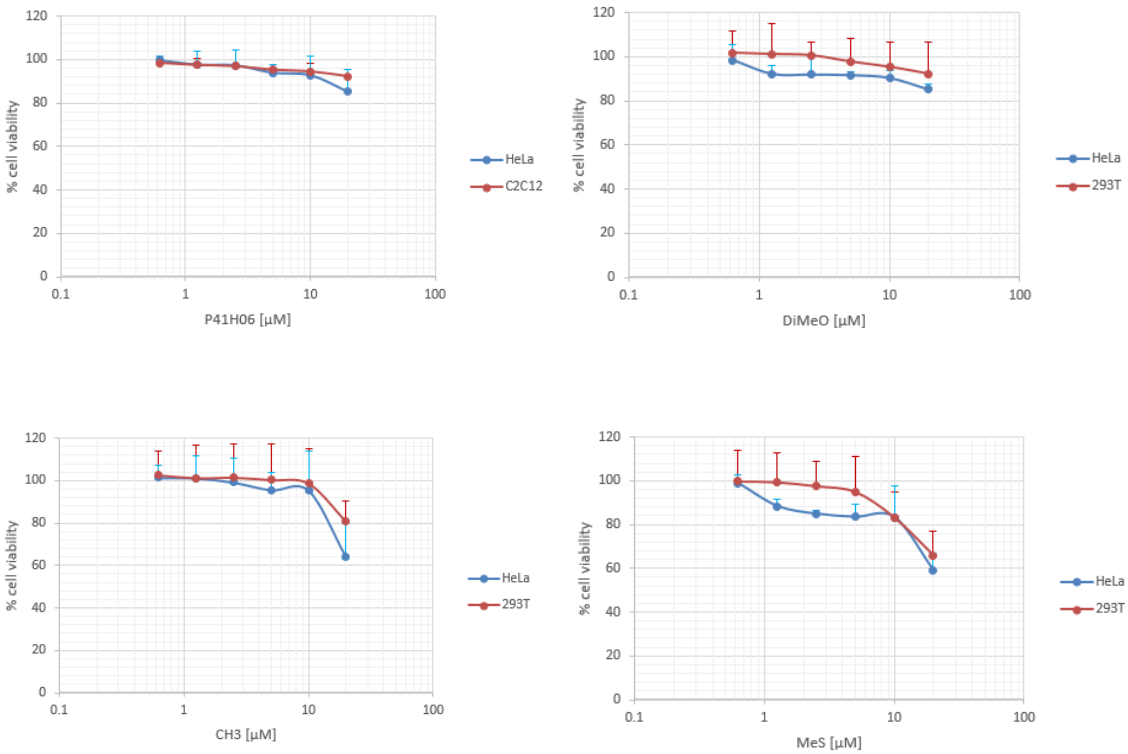

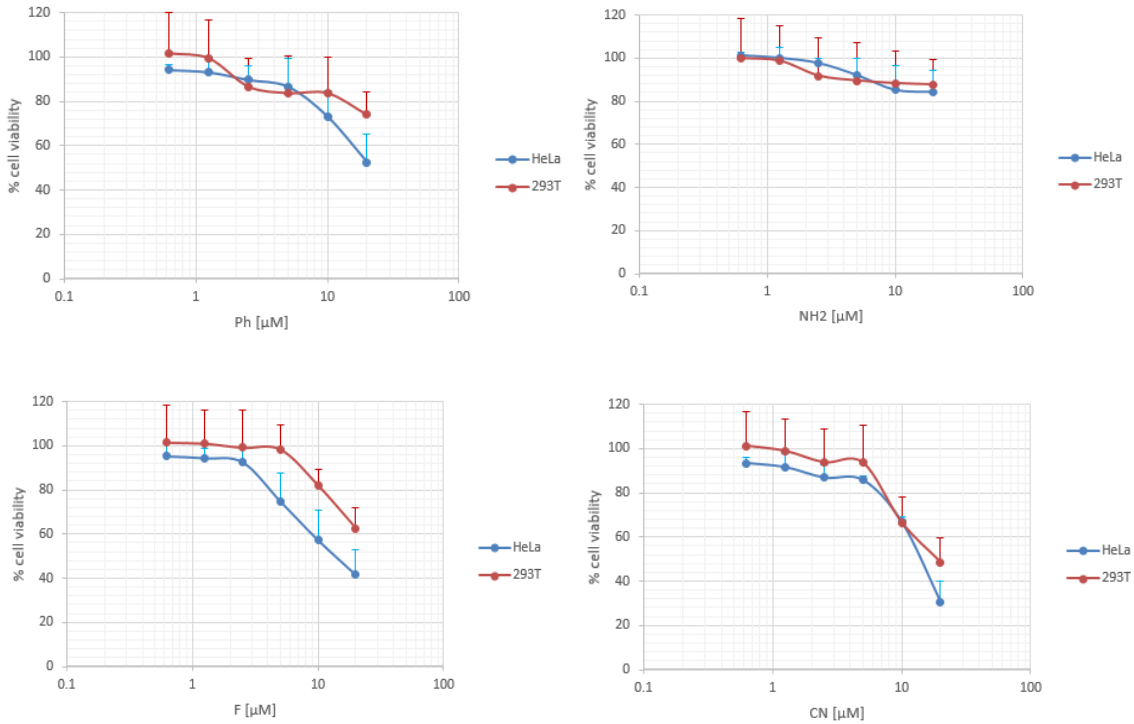

Fig. 8 Cell viability assay with compounds using 2 different cell lines, HeLa (human cervix adenocarcinoma) and 293T (human embryonic kidney). The cells were treated with various compounds for 24 h in a dose-dependent manner, and the cell viability was analyzed using an MTT assay. Treatment with CN and F, electron withdrawing functional groups at R_1 position exhibited ~60% cell death as opposed to ~20% cell death following DiMeO, P41H06, and CH3 functional group treatments.

2.4 Further optimization of hit compound

We were then interested to examine the structural and functional exploration of hit compound as an autophagy inducer (Fig. 3). Meta and para methoxy R_1 substituted compounds were synthesized to determine the effects of methoxy group at different position. Fig. 9 (a) shows the structural / biological activity analysis with structurally similar compounds. Based on the fluorescence images (Fig. 9 (b)), LD intensity after treatment with P41H6 is certainly different from that of P40C10, and a significant

reduction in LDs was visualized by SF44 under treatment with P41H06. On the other hand, autophagy inducing activities were lost when R_1 substituted methoxy group is moved to para or meta position, and even a higher level of cytotoxicity was observed with the treatment of P41H06M (Fig. 10). Through the cell viability assay using 2 different cell lines, HeLa (human cervix adenocarcinoma) cells and C2C12 (mouse myoblast) cells, we confirmed that P41H06 effects on autophagy are not caused by cytotoxicity (Fig. 10). With these results, P41H6O is the only compound that reduces cellular LDs, indicating that R_1 substituted methoxy functional group (P41H06) might play a significant role in autophagic process. Even though we couldn't find more potent compound than the hit in the effort of opitimization of hit compound structure, it was worth pointing out that potency is largely influenced by the chemical nature of the R_1 position and substituent.

(a)

P40C10

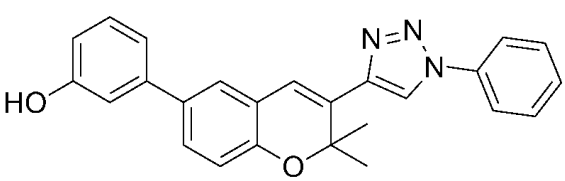

P41H06

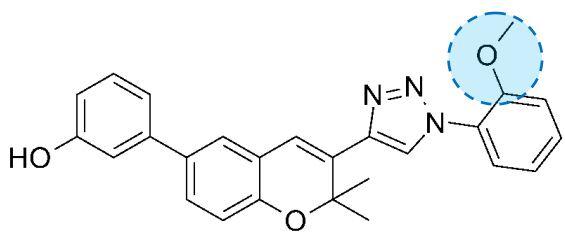

P41H06M

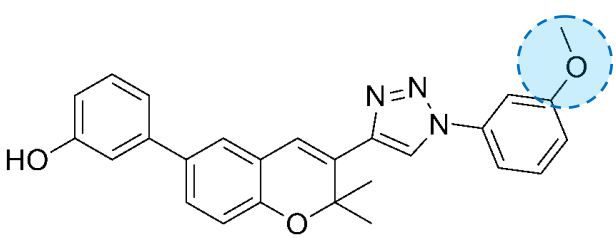

P41H06P

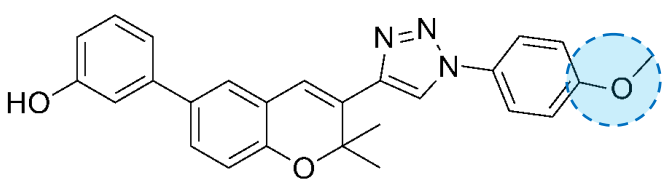

(b)

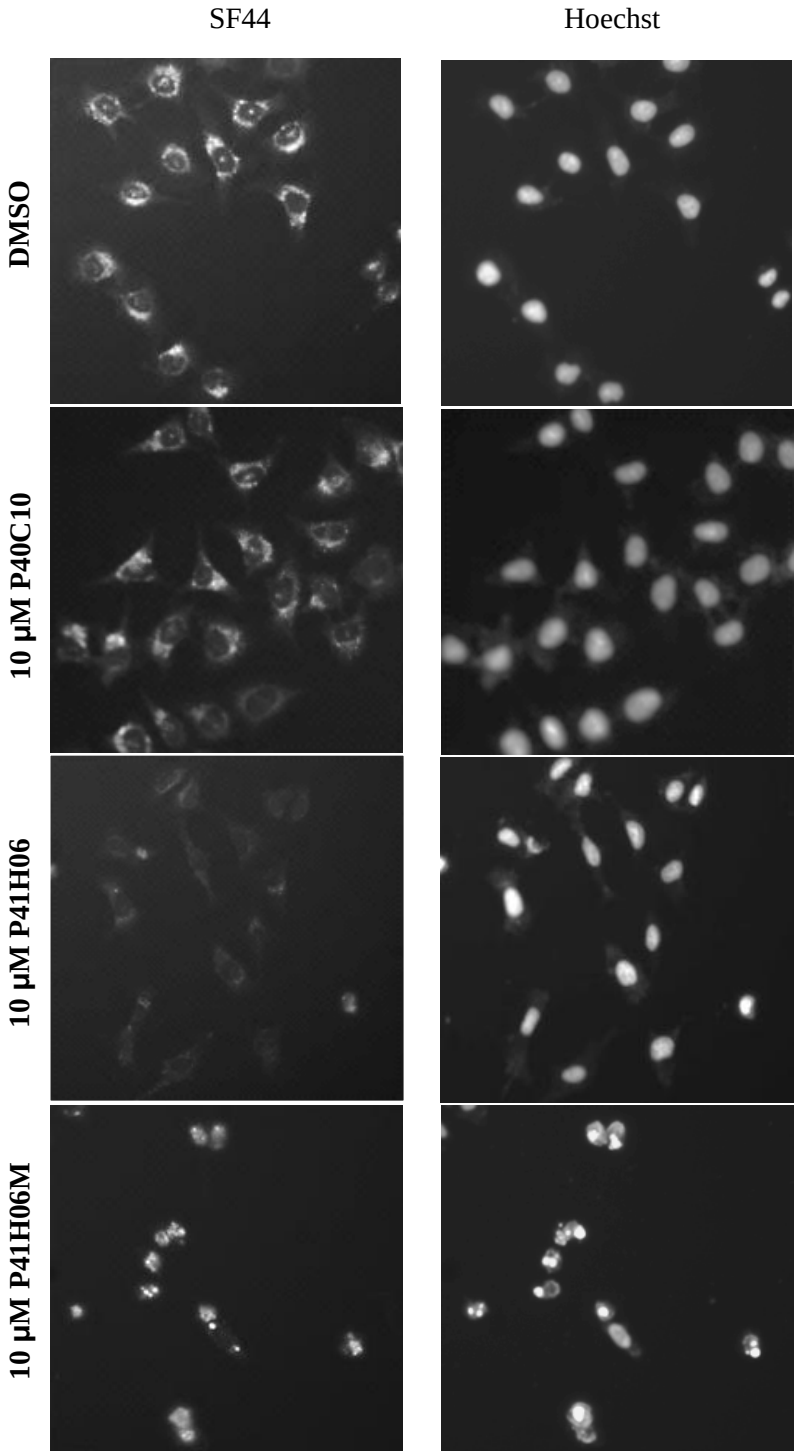

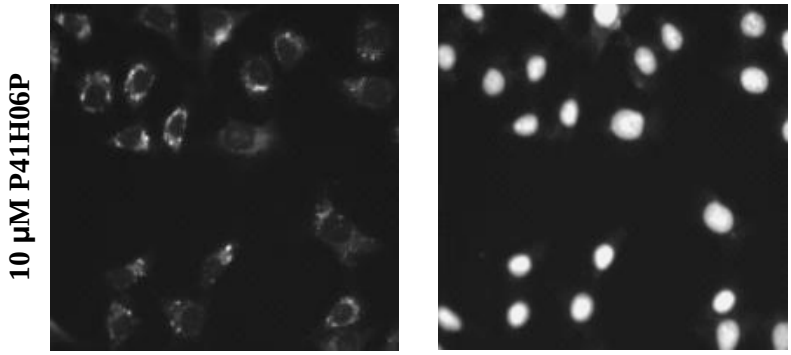

Fig. 9 Effect of chemical structure on autophagy inducing activity. (a) Chemical structure of compounds; P40C10, P41H06, P41H06M, and P41H06P. (b) Representative fluorescence images from InCell Analyzer 2000 (GE Healthcare): DMSO as control, 10 μM of P41H06, 10 μM of P40C10, 10 μM of P41H06M, and 10 μM of P41H06P. Images were visualized using SF44 (left) and Hoechst (right).

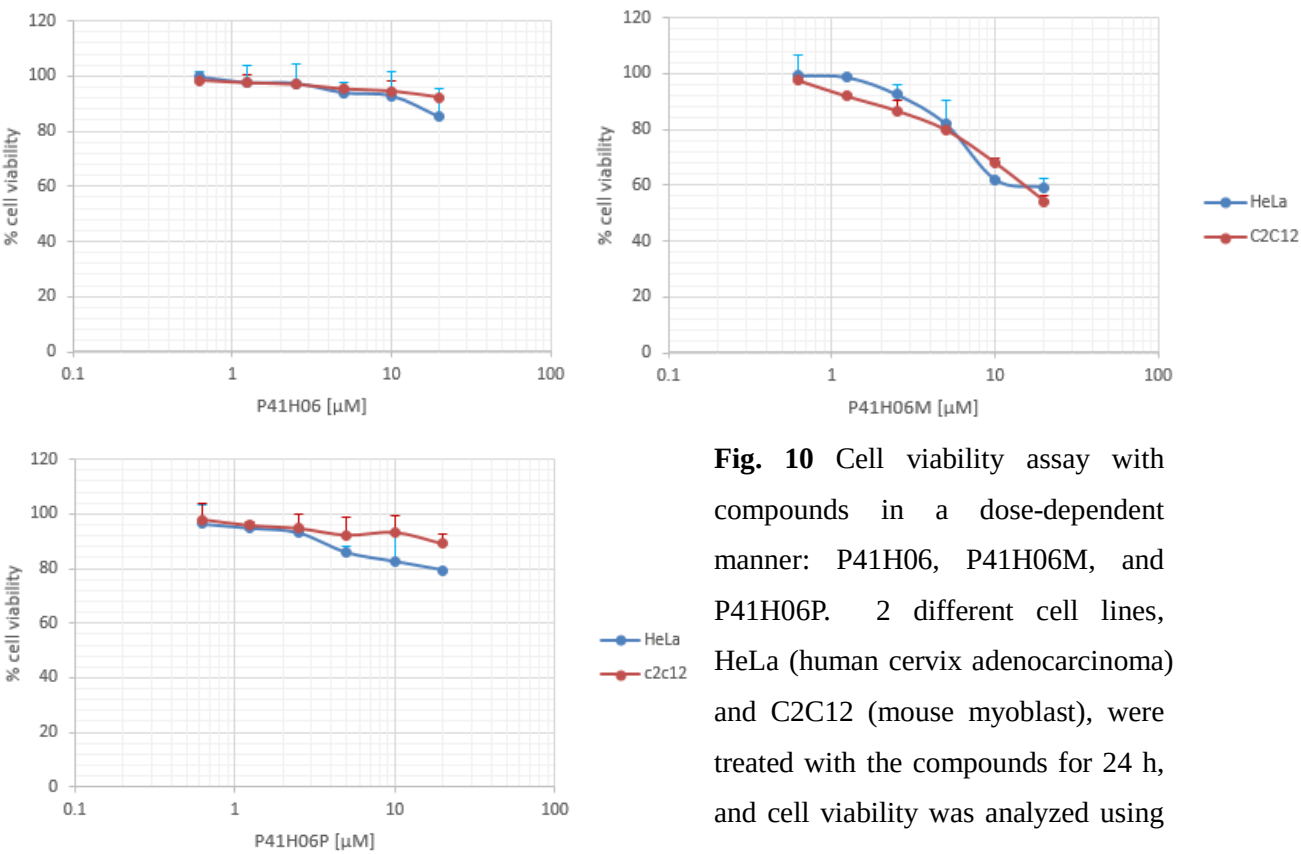

Fig. 10 Cell viability assay with compounds in a dose-dependent manner: P41H06, P41H06M, and P41H06P. 2 different cell lines, HeLa (human cervix adenocarcinoma) and C2C12 (mouse myoblast), were treated with the compounds for 24 h, and cell viability was analyzed using

an MTT assay. Treatment with P41H06 and P41H06P exhibited minimal cell death (<10%) as opposed to ~40% cell death following P41H06M treatment.

2.5 Detection of autophagome and autolysome formation events using mCherry-GFP-LC3 puncta assays

Besides novel LD screening, another useful and independent assay to confirm the measurement of autophagic substrate levels is to monitor autophagic flux by tracing mCherry-GFP-LC3 construct [31]. Although it requires transient transfection of autophagic flux reporter mCherry-GFP-LC3 tandem construct in HeLa cells, this assay allows distinction between autophagosomal and autolysosomal LC3B as yellow (indicating co-localization of GFP and mCherry) and red signals, respectively. It is based on the concept of the difference in the nature of two fluorescent proteins and acidification capacity of the lysosome. For example, mCherry fluorescence exhibits stable in acidic lysosome, whereas the fluorescent signal of GFP-labeled autophagic substrates LC3 is quenched inside the acidic lysosome due to low lysosomal pH so that only mCherry-LC3 can be readily detected in autolysosomes [30]. We therefore used mCherry-GFP-LC3 construct (gift from Dr. Heesun Cheong, National Cancer center) to further confirm our results by monitoring autophagic flux and determining LC3B localization. By DeltaVision microscope imaging, autolysosomes and autophagosomes are observed as red (mCherry) and yellow (mCherry and GFP), respectively, in control condition, suggesting that autophagosomes and autolysosomes remained intact (Fig 11(a)). When autophagy is induced, HeLa cells showed decreased green fluorescence intensity for LC3B and increased red (mCherry) puncta, indicating that autophagosomes were converting into autolysosomes (Fig. 11(b) and (d)); however, when maturation into autolysosomes is blocked by a late stage autophagy inhibitor, only the number of yellow punctae (mCherry and GFP) are increased (Fig. 11(c)). By tracing mCherry-GFP-LC3 construct, we confirmed the induction of autophagy following treatment with P41H06.

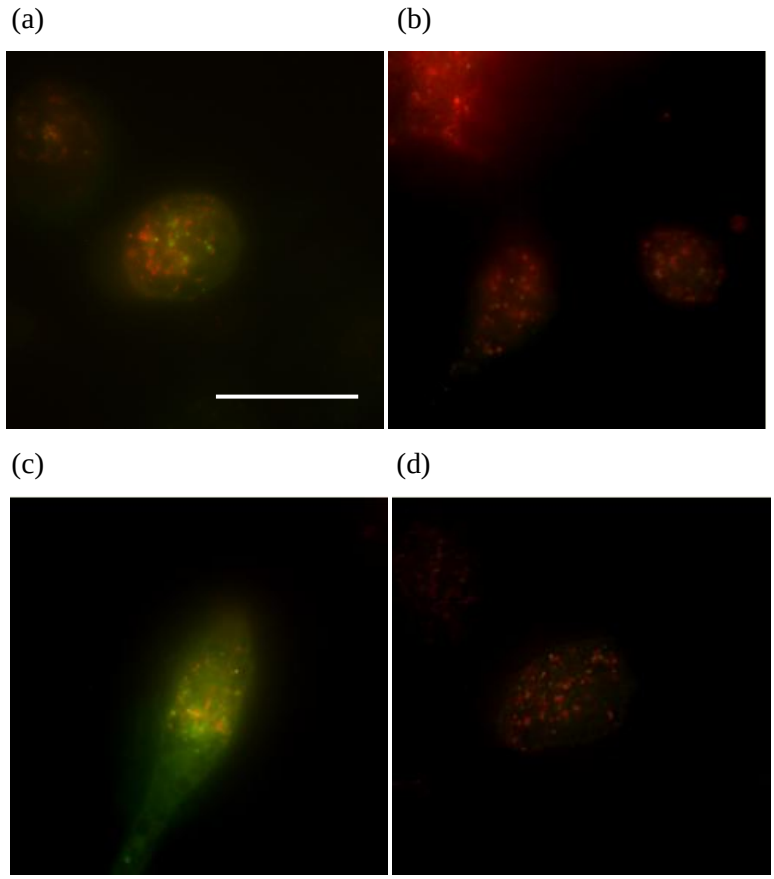

Fig. 11 Detection of autophagome and autolysome formation events with mCherry-GFP-LC3 construct. Representative fluorescence images of HeLa cells transiently expressing mCherry-GFP-LC3 from DeltaVision microscope, 100X. Fluorescent labeling of mCherry-GFP-LC3 allows differentiation between autophagosomes and autolysosome formation. At 24h after transfection, HeLa cells were treated for 6 h with (a) DMSO as a control, (b) 100 nM of rapamycin to induce autophagy; (c) 10 nM of bafilomycin A1 to block autophagosome fusion at late stage, and (d) 20 μM of P41H06. Autophagosomes and autolysosomes (lysosome fusion with autophagosome) are monitored and labeled with yellow (mCherry and GFP) and red (mCherry) puncta, respectively, in control by live cell imaging (a). Autophagy flux is increased with increased autolysosomses labeled with red (mCherry) signals by treatment of rapamycin and P41H06 ((b) and (d)). Bafilomycin A1 causes a

significant increase in GFP-LC3 yellow puntae by blocking fusion between autophagosome and lysosome (c). The scale bar represents 20 μm.

2.6 Mode of action of hit compound: P41H06-induced autophagy as an mTOR-independent autophagy

We next studied whether induction of autophagy by P41H06 was dependent on the known pathway that is negatively regulated by mTOR in mammalian cells. The induction of autophagy can be mediated by signaling through the mammalian target of rapamycin (mTOR) or through a complex of the class III phosphoinositide-3-kinase (PI3K) and Beclin-1(BECN1). mTOR is a negative regulator of autophagy and its chemical inhibition by rapamycin relieves this blockade.

To study the effects of P41H06 on mTOR activity, we examined the phosphorlyation of S6K, one of the mTOR substrates [32]. And, mTOR activity can be implied by the levels of phosphorylation of its substrates, ribosomal S6 protein kinase (p70S6K) and the phosphorylation of ribosomal S6 protein at Ser 235/236. S6K phosphorylation was dramatically suppressed by rapamycin treatment while its level had no such effects by treatment of P41H06, suggesting that P41H06 does not inhibit mTOR (Fig. 12(a)). Furthermore, blockage of autopagosome-lyssosome fusion via baflomycin A1 [33] resulted in the expected increase in LC3 II in HeLa.

The PI3K signaling can activate autophagy independently of mTOR inhibition by induction of Beclin. And, the high expression of Beclin 1 induces autophagy by promoting autophagosome formatting when in complex with Vps34 (vacuolar protein sorting 34)/ classIII PI3K [34]. To determine which of these was responsible for increased autophagy, Beclin 1 was analyzed as sign of mTOR-independent autophagy because it is essential in the formation of autophagosome. The stimulation of autophagy by rapamycin did not alter the expression level of Beclin 1, its importance for controlling the autophagic pathway. Surprisingly, P41H06 treated cells showed a small increase in the expression of Beclin-1 protein. These results indicated that enhanced levels of

autophagy with P41H06 treatment were mediated by mildly increased Beclin-1 expression (Fig. 12(a)).

Taken together, the induction of autophagy with treatment of P41H06 is not mediated by signaling through the AKT-mTOR-S6K1 pathway, but rather by Beclin-1, a crucial regulator of autophagosome formation which forms a protein complex with the class III PI3K.

Since P41H06 induces autophagy independently of mTOR inhibition, we predicted that co-treatment of P41H06 and rapamycin would facilitate greater degradation of p62 degradation and greater conversion of LC3 I to LC3 II, compared with the single either compound alone. As expected, co-treatment of P41H06 and rapamycin had additive effect in increasing p62 degradation (Fig. 12(b)). Thus, autophagic activity can be further enhanced through simultaneous induction of mTOR-dependent and mTOR-independent route, where mTOR-independent autophagy pathway is induced by P41H06 and mTOR-dependent autophagy pathway is induced by rapamycin individually. In addition, co-treatment of P41H06 with bafilomycin Al significantly increased p62 accumulation, strongly arguing that the increased autophagosomes induced by P41H06 are upstream of autophagosome-lysosome fusion, and bafilomycin blocks atuophagic flux.

(a)

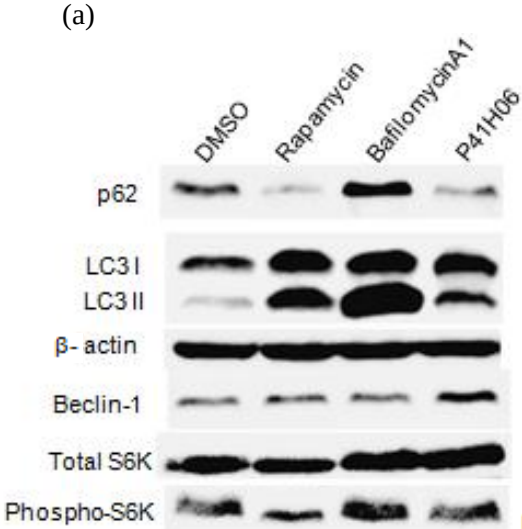

(b)

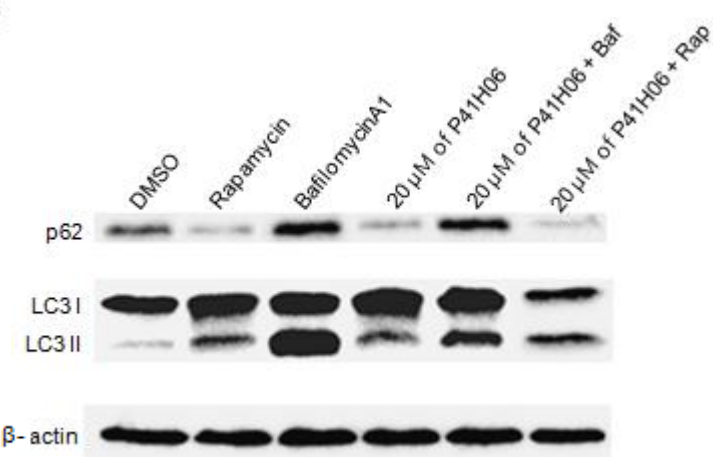

Fig. 12 Mode-of-action study of P41H06. (a) Mechanism of action of P41H06 toward mTOR-dependent and independent pathway. Western blotting analysis of Beclin-1 and phospho-S6K. (b) Co-treatment assay via western blot analysis. HeLa cells were treated with 20 μM of P41H06, 10 nM of bafilomycin A1, and 100 nM of rapamycin for 6 h. Treatment with 100 nM of rapamycin and 10 nM of bafilomycinA1 were used as positive and negative controls, respectively. Phospho-S6K indicates phosphorylated forms of S6K.

2.7 P41H06-induced autophagy in NSC-34 motor neuron cell line

There is supporting observations that deregulated autophagy might involve in ALS, and mutant superoxide dismutase 1(SOD1G93A) is degraded by induction of autophagy in disease and cell model of ALS [35]. And, we proposed that our novel mTOR-independent autophagy inducer can stimulate a natural defense system in motor neurons by removing all of the disease-causing proteins, SOD1 in motor neurons to reduce neurodegeneration [36]. Since ALS is a progressive neurodegenerative disease that primarily affects motor neurons, we first tested for efficacy of P41H06 in NSC-34 motor neuron cells (gift from Prof. Jung-Joon Sung, Seoul National University Hospital) by measuring the levels of LC3 and p62. The NSC-34 cell line is a mouse neural hybrid cell between neuroblastoma and spinal cord cells which resembles developing motor neurons *in vitro* [37]. Consistent with the previous observations in HeLa cells, the turnover of autophagic marker LC3 II increased also in NSC-34 cells treated with P41H06 for 12h, which was accompanied with p62 reduction (Fig. 13). Treatment with Bafilomycin A1 resulted in the expected increase in LC3 II but inhibited degradation of p62. These results suggest that in response to treatment of P41H06 autophagy is induced in NSC-34 cells, whi actin ould be responsible for the degradation of mutant proteins, such as SOD1G93A, the hallmarks of ALS.

We hope to study the degradative and dysregulated autophagy pathway can be

induced by P41H06 in the mutant SOD1G93A cell model of ALS, thereby enhancing survival in motor neuron harboring mutant SOD1 for ALS and related disease conditions. To determine if increasing autophagy is beneficial to the progression of ALS, our lab began studies to see the effects of mutant SOD1G93A on autophagic activity in cells by administering our autophagy activating compound.

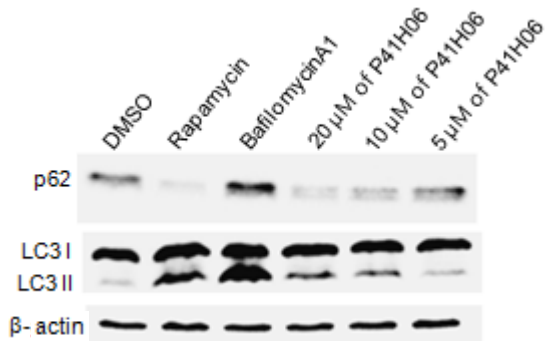

Fig. 13 Regulation of autophagy in NSC-34 motor neuron cells. NSC34 cells were treated with 100 nM of rapamycin (positive control), 10 nM of bafilomycinA1 (negative control), and 20 μM of P41H06 at various doses for 12 h.

2.8 Real-time monitoring of SOD1-EGFP fusion protein in cell model of ALS

Protein inclusions of mutant SOD1G93A due to misfolding have been found in tissues from ALS patients, animal and cell models [38,39] because mutant SOD1 aggregation is known to toxic for the cell via several mechanisms that include dysfunction of organelles, e.g., mitochondria, induction of oxidative stress, impairment of proteasome function [40]. Since mutant SOD1G93A has been shown to be degraded by autophagy in cell models of ALS [41], we thought that P41H06 can reduce protein aggregate formation by inducing autophagy in cell model of ALS. In order to mimic the pathology of mutant SOD1G93A aggregates associated familial ALS [42] to test potential therapeutic compound, 293T cell line was transiently transfected with human wtSOD1-EGFP or mtSOD1G93A-EGFP. Then, a single cell was tracked, and time-

lapse live cell imaging was carried out using a DeltaVision microscope. The cells expressing human wtSOD1 showed a widespread fluorescence in the cytoplasm (Fig.13(a)), whereas in the cells transfected with human mtSOD1G93A-EGFP large and prominent cytoplasmic protein aggregates were observed (Fig.13(b)). By caring out the time-lapse live cell imaging, however, those aggregates were reduced in the presence of 200 nM Rapamycin or 20 μM P41H06 (Fig.13(c) and 13(d)). Aggregate formation and mutant SOD1 were significantly decreased in the presence of P41H06 in cell model of ALS possibly due to its capacity to induce autophagy (Fig.13(d)). This experiment has shown that P41H06 can prevent protein aggregation that is common in neurodegenerative disease.

Fig. 14 Time-lapse of SOD1-EGFP fluorescence images from DeltaVision Microscope, 60X. HEK293T cells were transiently transfected with vector pEGFP-N1(Clontech) encoding mouse wtSOD1 linked at the C-terminus to the enhanced green fluorescent protein tag (wtSOD1-EGFP) and mutant SOD1G93A with the same tag (mtSOD1G93A-EGFP)(gift from Prof. Jung-Joon Sung, Seoul National University Hospital) , using Lipofectamine LTX plus 2000 (Invitrogen). mtSOD1G93A-EGFP formed large aggregates in the cytoplasm of live HEK293T cells. At time O h, HEK293T cells, expressing mtSOD1G93A-EGFP, were treated with either 200 μM of rapamycin or 20 μM of P41H06 up to 5h. The scale bar represents 25μm.

Fig 14. Time 0 h

3. Conclusion

The study of autophagy has recently drawn tremendous attention due to its mechanism and significance in human health. Therefore, there is a great interest in identifying specific autophagy modulators. The fact that various contents from a single cell could be obtained and allows the valuable information, HCS has received enormous attention. However, experimental HCS methods to identify autophagy modulators are limited by the lack of methods to specifically quantify each step of the autophagic pathway. Monitoring of atuophagic flux is therefore required for the robust interpretation of autophagic activity. Our group has constructed HCS monitoring system of cellular LDs as a marker of autophagic process that can discriminate the effects of autophagy modulators. The ability to measure relative impacts on different pathway events revealed striking conditional differences between the most commonly used drug modulators of autopahgy. The unique fluorescent property of SF44 enables specific and selective staining of hydrophobic LDs, and thereby autophagic flux can be measured with cellular LD levels as a late stage marker of autophagy [3]. The advantage of our HCS platform is that false-positive can be eliminated because the image anaysis results can be filtered along with the cell morphology and cell toxicity before moving forward into further study. Furthermore, our phenotype-based monitoring method allows rapid LD staining of fluorescent probe and does not require any genetic perturbations. Therefore, this approach was highly scalable, allowing for quantitative library screening of about 1,440 small-molecule compounds. After conducting HCS with in-house library, we identified a small-molecule autophagy inducer, P41H06. We further validated the impact of the compound as novel inducer on autophagic activity using fluorescent protein-based sensor, mCherry-GFP-LC3, in order to simultaneously monitor autophagosome and autolysosome. Mechanism-of-action study clearly indicated that P41H06 induces autophagy in an mTOR-independent manner by increasing the levels of autophagy regulators, Beclin-1. We also discussed the possible implications of autophagy inducer in cellular ALS models that the autophagy induction mitigates neurodegeneration

by acting directly on mutant SOD1 clearance, which can be potential therapeutic approaches for ALS. Thus our phenotype-based HCS method is effective and will be informative for the growing field as research tools and developing drugs for autophagy-related diseases such as Alzheimer's and Lou Gehrig's diseases, for which there have been many failures of target-based drug candidates in clinical trials.

4. Experimental Procedures

Cell culture HeLa (human cervical adenocarcinoma) cells were obtained from American Type Culture Collection and cultured in RPMI 1640 supplemented with 10 % (v/v) fetal bovine serum and 1 % (v/v) antibiotic-antimycotic solution. NSC-34 (mouse motor neuroblastoma) cells, C2C12 (mouse myoblast) cells, and HEK293T (human embryonic kidney) cells were grown in Dulbecco's modified Eagle's medium-high glucose (DMEM; Gibco), supplemented with 10 % (v/v) fetal bovine serum and 1 % (v/v) antibiotic-antimycotic solution. NSC-34 cells were grown in Dulbecco's modified Eagle's
medium-high glucose (DMEM; Gibco), supplemented with 10% fetal bovine serum , 100 units/ml penicillin and 0.1 mg/ml streptomycin (Invitrogen). Cells were maintained in a humidified atmosphere of 5 % CO2 incubator at 37 ℃ and cultured in 100 mm cell culture dish.

Construction of high content screening platform and automated data analysis For the image-based screening in a high-throughput manner, HeLa cells were seeded on a 96-well plate with clear bottom and black well. Using 96 solid pin multi-blot replicators, various compounds from our in-house chemical library were transferred to individual wells of a 96 well plate with their final concentration as 10 μM. Individual screening plates contained oleic acid as a positive control, serum free condition as a negative control, and DMSO as a vehicle. After 24 h incubation at 37 ℃, SF44 (5 μM) and Hoechst 33342 (2 μg/ml) was added in individual wells. Serum free condition for negative control was needed to exchange its media with regular media before the treatment of SF44 and Hoechst. After 30 min incubation, automatic fluorescence imaging of designated plates was performed with InCell Analyzer 2000 (GE Healthcare) without any washing steps. Images of randomly selected 4 different spots per individual well in a 96-well plate were automatically captured. Images were taken by auto-focusing mode and 20x scale. Fluorescence imaging was also performed with SF44

for lipid dropet (LD) and Hoechst for nuclei at the indicated filter setting; Excitation filter: 430/24x and Emission filter 605/64 nm for LD; Excitation filter: 350/50x and Emission filter: 455/50 nm for nuclei. Data were analyzed by InCell Analyzer 1000 workstation 3.6 program according to the manufacturer's protocol. Fluorescence intensity of LD was interpreted as a cellular organelle using granularity module and the area of individual cell was recognized by nuclei staining using collar segmentation.

Visualization of lipid droplet in live cells using SF44 HeLa cells were seeded on a coverglass bottom dish and incubated in 5 % CO2 incubator at 37 ℃ overnight. Those cells were subjected to the chemical treatment or autophagy inducing stimuli. Cells were incubated 6 h with 100 nM of rapamycin to activate autophagy, 10 nM of bafilomycin A1 to inhibit autophagy, DMSO as a vehicle, 5 μM of oleic acid as a positive control, and 20 μM of P41H06. For LD visualization, the media were replaced with fresh media containing 5 μM of SF44. After 10 min incubation at 37 ℃, Hoechst 33342 (2μg/ml) was added to cells, and the cells were further incubated for 20min. LD staining pattern in live cells were measured using fluorescence microscopy directly without additional washing steps. Fluorescence microscopy studies were carried with Olympus Inverted Microscope Model IX71, equipped for epi-illumination using a halogen bulb (Philips No. 7724). Emission signal of each experiment was observed at the indicated spectral setting: green channel, using a 450–480 band pass exciter filter, a 500 nm center wavelength chromatic beam splitter, a 515 nm-long pass barrier filter (Olympus filter set U-MWB2). Emission signal of each experiments were detected with 12.5M pixel recording digital color camera (Olympus, DP71).

Western blot analysis HeLa cells were seeded on 6 well plates and incubated in 5 % CO2 incubator at 37 ℃ overnight. Cells were treated with hit compounds at various concentrations. In case of co treatment assay, cells were treated with 20 μM of each compound in the presence of either 10 nM of bafilomycin A1 or 100 nM of rapamycin. After 6 h incubation with individual compounds, cells were washed by PBS and harvested. Cell lysates were obtained by 20 min treatment with RIPA or RIPA-P cell lysis buffer containing protease inhibitors and phosphatase inhibitors at ice. After the

centrifugation of cell lysates at 15,000 rpm and 4 ℃ for 10 min, the protein concentration in the supernatant was measured by BCA assay kit, purchased from PIERCE. The resulting proteome were analyzed by SDS-PAGE and transferred into PVDF membrane, followed by 2% BSA blocking in TBST over 1 h. The samples were subjected to immunoblotting to detect with specific primary antibodies, e.g. anti-LC3 (abcam), anti-p62 (cell signaling), anti-β-actin (cell signaling), anti-p70 S6 kinase (phospho T389) (abcam), anti-Beclin-1(cell signaling), and anti-SOD1(abcam). Specific antibodies were treated for overnight at 4 ℃, followed by washing with TBST for 1h. The resulting membrane was exposed into HRP conjugated secondary antibody for 1 h at room temperature. After 1 h washing with TBST, the membrane was developed by ECL prime solution (GE Healthcare Life Science) and the chemiluminescent signal was measured by ChemiDoc MP imaging system. To investigate the mode of action of P41H06, individual proteome samples were prepared by identical procedure after treatment of P41H06 (20μM) for designated time frames. The procedure of western blot assay was identical with an above-mentioned procedure except for primary antibodies.

Detection of mCherry-GFP-LC3 puncta HeLa cells were seeded on 8 chambered cover glass bottom dish and incubated at 37 ℃ for overnight. The cells were transfected with mCherry-EGFP-LC3 (gift from Korea National Cancer Center) using Lipofectamine LTX and PLUS reagents (Life Technologies). Then, the cells were treated with the specified concentration of the compounds or DMSO as a control for 6 h. After 6 h incubation, image stacks were taken using a DeltaVision deconvolution fluorescent microscope (GE Healthcare) fitted with a 100X objective, deconvoloved and projected using SoftWorx 2.50 software (Applied Precision).

Real-time monitoring of SOD1-EGFP fusion protein HEK293T cells were seeded on 8 chambered cover glass bottom dish and incubated at 37 ℃ for overnight. Te cells were transfected with wtSOD1-EGFP and mtSOD1G93A-EGFP (gifts from Prof. Jung-Joon Sung, Seoul National University Hospital) using Lipofectamine LTX and PLUS reagents (Life Technologies). Then, the cells were treated with the specified concentration of the compounds or DMSO as a control, and

then time-lapse fluorescence images were taken from DeltaVision deconvolution fluorescent microscope (GE Healthcare) fitted with a 60X objective, deconvoloved and projected using SoftWorx 2.50 software (Applied Precision).

Cell viability test To estimate the effects of the compounds on cell viability, HeLa, HEK293T, and C2C12 cells were seeded in 96-well plates in 100 μL and cultured for 24 h at 37℃ in a 5% CO2 incubator. After incubation, the cells were treated with the indicated concentrations for 24 h. After 24h treatment, 10 μL of EZ-Cytox Cell Viability Assay solution WST-1® (Daeil Lab Service, Jong-No, Korea) was added to each well, and the cells were then incubated for 3 h at 37℃ in a 5% CO2. Absorbance was measured at 460 nm with an ELISA reader (Molecular Devices, Sunnyvale, CA, USA).

Reagents and materials Chemicals for autophagy regulation were purchased from Sigma-Aldrich. Fluorescent dyes such as SF44 and Hoechst 33342 were obtained by reported procedure1 or purchased from Invitrogen. Micro BCA Protein Assay Kit was purchased from PIERCE and was used for the measurement of protein concentration of cell lysate. Cell culture reagents including fatal bovine serum, culture media, and antibiotic-antimycotic solution were purchased from GIBCO, Invitrogen. The culturing dish or screening plates were purchased from CORNING. All antibodies for western blot analysis were purchased from Abcam and Cell Signalling. Developing for western blot analysis was performed by Amersham ECL Prime Western Blotting Detection System from GE Healthcare Life Science.

Acknowledgements We thank: Dr. Heesun Cheong, National Cancer center, for the mCherry-GFP-LC3 plasmid; Prof. Jung-Joon Sung, Seoul National University Hospital, for the human wild type SOD1-GFP, human mutant G93A SOD1-EGFP, and NSC-34 cells.

5. References

[1] D.C. Rubinsztein, *et al*. Autophagy modulation as a potential therapeutic target for diverse diseases. *Nat Rev Drug Discov.* 2012 Sep. **11(9)**: 709–730.

[2] A.R. Winslow and D.C. Rubinsztein. Autophagy in neurodegeneration and development. *Biochim Biophys Acta.* 2008 Dec. **1782(12)**: 723–729.

[3] S. Lee, E. Kim, and S.B. Park. Discovery of autophagy modulators through the construction of a high-content screening platform via monitoring of lipid droplets. *Chem. Sci*. 2013. **4**: 3282-3287.

[4] A.Criollo, M.C. Maiuri, E. Tasdemir, *et al*. Regulation of autophagy by the inositol trisphosphate receptor. *Cell Death Differ.* 2007. **14**: 1029–1039.

[5] N. Mizushima and D.J. Klionsky. Protein turnover via autophagy: Implications for metabolism. *Annu. Rev. Nutr.* 2007. **27**: 19–40.

[6] N. Mizushima. Autophagy: process and function." *Genes Dev.* 2007. **21(22)**: 2861–2873.

[7] Y. Kabeya, N. Mizushima, T. Ueno, *et al.* LC3, a mammalian homologue of yeast Apg8p, is localized in autophagosome membranes after processing. *EMBO J.* 2000. **19(21)**: 5720-5728.

[8] A. Puissant, N. Fenouille, and P. Auberger. When autophagy meets cancer through p62/SQSTM1. *Am J Cancer Res.* 2012. **2(4)**: 397-413.

[9] J.P. Taylor, J. Hardy, and K.H. Fischbeck. Toxic proteins in neurodegenerative disease. *Science*. 2002. **296(5575)**:1 991–1995.

[10] A. Williams, L. Jahreiss, S. Sarkar, *et al.* Aggregate-prone proteins are cleared from

the cytosol by autophagy: therapeutic implications. *Curr Top Dev Biol.* 2006. **76**: 89–101.

[11] M. Urushitani, J. Kurisu, K. Tsukita, *et al*. Proteasomal inhibition by misfolded mutant superoxide dismutase 1 induces selective motor neuron death in familial amyotrophic lateral sclerosis. *J Neurochem.* 2002. **83(5)**: 1030–1042.

[12] B. Ravikumar, R. Duden, and D.C. Rubinsztein. Aggregate-prone proteins with polyglutamine and polyalanine expansions are degraded by autophagy. *Hum Mol Genet.* 2002. **11(9)**: 1107–1117.

[13] J.L. Webb, B. Ravikumar, J. Atkins, *et al.* Alpha-synuclein is degraded by both autophagy and the proteasome. *J Biol Chem.* 2003. **278(27)**: 25009–25013.

[14] A.D. Balgi, B.D. Fonseca, E. Donohue, *et al.* Screen for chemical modulators of autophagy reveals novel therapeutic inhibitors of mTORC1 signaling. *PLoS One.* 2009. **4**: e7124.

[15] J.J. Burbaum and N.H. Sigal. New technologies for high-throughput screening. *Curr Opin Chem Biol.* 1997. **1**: 72–78.

[16] C.M Crews and U. Splittgerber. Chemical genetics: exploring and controlling cellular processes with chemical probes. *Trends Biochem Sci.* 1999. **24**: 317–320.

[17] L. Zhang, J. Yu, H. Pan, *et al*. Small molecule regulators of autophagy identified by an image-based high-throughput screen. *Proc Natl Acad Sci U S A.* 2007 Nov 27. **104(48)**: 19023-8.

[18] P. Hundeshagen, A. Hamacher-Brady, R. Eils, *et al.* Concurrent detection of autolysosome formation and lysosomal degradation by flow cytometry in a high-content screen for inducers of autophagy. *BMC Biology.* 2011. **9**: 38.

[19] E. Gregori-Puigjane, *et al*. Identifying mechanism-of-action targets for drugs and probes. *Proc Natl Acad Sci U S A.* 2012. **109**: 11178–11183.

[20] N. Chen and J. Debnath. Autophagy and tumorigenesis. *FEBS Lett.* 2010 Apr 2. **584(7)**: 1427–1435.

[21] S.J. Buss, S. Muenz, J.H. Riffel, *et al*. Beneficial effects of Mammalian target of rapamycin inhibition on left ventricular remodeling after myocardial infarction. *J Am Coll Cardiol.* 2009 Dec 15. **54(25)**: 2435-46

[22] J.B. Easton and P.J. Houghton. mTOR and cancer therapy. *Oncogene.* 2006. **25**: 6436–6446.

[23] N.S. Heaton and G. Randall. Dengue virus induced autophagy regulates lipid metabolism. *Cell Host Microbe.* 2010 Nov 18. **8(5)**: 422–432.

[24] R. Singh, S. Kaushik, Y. Wang, *et al*. Autophagy regulates lipid metabolism. *Nature*. 2009 Apr 30. **458(7242)**: 1131-5.

[25] D.C. Rubinsztein DC, *et al*. In search of an autophagomometer. *Autophagy* .2009. **5**: 585–589.

[26] A.S. Greenberg, R.A. Coleman, F.B. Kraemer, *et al*. The role of lipid droplets in metabolic disease in rodents and humans. *Journal of Clinical Investigation.* 2011. **121(6)**: 2102–2110.

[27] R. Singh and A.N. Cuervo. Lipophagy: Connecting Autophagy and Lipid Metabolism. *International Journal of Cell Biology.* 2012. Article ID 282041, 12 pages.

[28] E. Kim, S. Lee, and S.B. Park. A Seoul-Fluor-based Bioprobe for Lipid Droplets and Its Application in Image-based High Throughput Screening. *Chem. Commun*. 2012. **48(17)**: 2331-2333.

[29] Y. Kabeya, N. Mizushima, T. Ueno, *et al*. LC3, a mammalian homologue of yeast Apg8p, is localized in autophagosome membranes after processing. *EMBO J.* 2000. **19**: 5720–8.

[30] N. Mixushima, T. Yoshimorim, and B. Levine. Methods in Mammalian Autophagy Research. *Cell.* 2010 Feb 5. 140(3): 313–326.

[31] S. Kimura, T. Noda, and T. Yoshimori. Dissection of the autophagosome maturation process by a novel reporter protein, tandem fluorescent-tagged LC3. *Autophagy.* 2007. **3**: 452–460.

[32] T. Schmelzle and M.N. Hall. Tor, a central controller of cell growth. *Cell.* 2000 Oct 13. ***1*03(2)**: 253–262.

[33] A. Yamamoto, Y. Tagawa, T. Yoshimori, *et al.* Bafilomycin A1 prevents maturation of autophagic vacuoles by inhibiting fusion between autophagosomes and lysosomes in rat hepatoma cell line, H-4-II-E cells. *Cell Struct. Funct*. 1998. **23(1)**: 33–42.

[34] H. Rikiishi. Novel Insights into the Interplay between Apoptosis and Autophagy. *International Journal of Cell Biology.* 2012. Article ID 317645, 14 pages.

[35] T. Kabuta, Y. Suzuki, and K. Wada. Degradation of amyotrophic lateral sclerosis linked mutant Cu,Zn-superoxide dismutase proteins by macroautophagy and the proteasome." *J. Biol. Chem.* 2006. **281**: 30524–30533.

[36] S. Chen, X. Zhang, L. Song, *et al*. Autophagy dysregulation in amyotrophic lateral sclerosis. *Brain Pathol*. 2012. **22(1)**: 110–116.

[37] N.R. Cashman, H.D. Durham, J.K. Blusztajn, *et al*. Neuroblastoma×spinal cord (NSC) hybrid cell lines resemble developing motor neurons. *Dev. Dyn.* 1992. **194(3)**: 209–221.

[38] J.A. Johnston, M.J. Dalton, M.E. Gurney, *et al.* Formation of high molecular weight complexes of mutant Cu,Zn-superoxide dismutase in a mouse model for familial amyotrophic lateral sclerosis. *Proc. Natl. Acad. Sci.* 2000. **97:** 12571–12576.

[39] E. Kabashi and H.D. Durham. Failure of protein quality control in amyotrophic

lateral sclerosis, Biochim. *Biophys. Acta.* 2006. **1762:** 1038–1050.

[40] M. Urushitani, J. Kurisu, K. Tsukita, *et al.* Proteasomal inhibition by misfolded mutant superoxide dismutase 1 induces selective motor neuron death in familial amyotrophic lateral sclerosis. *J. Neurochem*. 2002. **83:** 1030–1042.

[41] T. Kabuta, Y. Suzuki, and K. Wada. Degradation of amyotrophic lateral sclerosislinked mutant Cu,Zn-superoxide dismutase proteins by macroautophagy and the proteasome. *J. Biol. Chem.* 2006. **281:** 30524–30533.

[42] N.R. Cashman, H.D. Durham, J.K. Blusztajn, *et al.* Neuroblastoma×spinal cord (NSC) hybrid cell lines resemble developing motor neurons. *Dev. Dyn.* 1992. **194:** 209–221.

국문초록

지방방울 바이오프로브와 고효율 이미지 기반 스크리닝 시스템을 통한 자가포식 저분자 조절 물질 개발

서울대학교 대학원

화학부 생화학 전공

유 빈

이 논문에서는 자가포식의 조절을 통해 세포의 운명을 제어할 수 있는 저분자 화합물에 관한 연구를 기술하였다. 자가포식은 세포의 불필요하거나 손상된 물질을 분해해 재활용하는 주요 시스템이며, 단백질 대사에도 깊이 관여하고 있다. 이 시스템은 생물체의 생존과 항상성을 유지해주는 중요한 역할을 한다. 자가포식의 조절이 제대로 되지 않거나, 노화, 유전적 변이, 스트레스 등으로 세포를 위협할 수 있는 변성 단백질이 누적 됐을 경우 신경세포가 손상되어 알츠하이머 병, 루게릭 병과 같은 퇴행성 뇌 질환뿐만 아니라 각종 신경성 질환을 일으킨다.

세계적으로 퇴행성 뇌 질환에 대한 연구가 많이 진행되고 있지만, 신경퇴행성 질환의 유발을 억제하는 치료제는 아직 발굴하지 못하였다. 이 논문에서는 표현형을 기반으로 한 스크리닝(phenotype-based screening)을 통하여 자가포식을 조절할 수 있는 저분자 화합물을 찾고, 이 화합물이

특별히 루게릭 병의 세포 모델에 미치는 효과를 검증한 연구에 대해 기술하였다.

자가포식을 조절하는 저분자 화합물을 탐색하기 위하여 기존에 알려진 고효율 이미지 기반 스크리닝 시스템(High-throughput image-based screening system)을 활용하였다. 이 시스템은 형광 프로브, Seoul-Flour 44(SF44)를 사용하여 세포 내의 중성지질 저장소인 지방 방울 (Lipid droplet)을 선택적으로 염색 함으로써 지방대사와 자가포식을 효율적으로 모니터링 할 수 있다. 이 시스템을 활용하여 대략 1440 개의 저분자 화합물 라이브러리를 스크리닝 하였고 지방 방울을 조절하는 후보물질을 발굴하였다. 나아가 이 화합물을 통해 자가포식을 조절하는 메커니즘을 규명하였으며, 구조-활성 상관관계(structure-activity relationship)를 연구함으로써 물질의 효능을 증진시킬 수 있는 구조적 특징을 파악하였다.

더 나아가 축적된 변성 단백질이 루게릭 병의 경우 SOD1 유전자에 변이가 일어나 SOD1 단백질이 축적됨으로써 운동성 신경세포를 사멸시키는 기작을 가지고 있으므로 루게릭 병의 *in vitro* 세포 모델(G93A-SOD1 cell model of ALS)을 통해 새롭게 발굴한 화합물이 루게릭병의 대표적 유발 축적 단백질인 mutant SOD1 을 감소시킴을 확인하였다.

이 화합물이 자가포식을 촉진하여, 추후 *in vivo* 실험으로 통해 루게릭 병의 대표적 유전 발병인자인 돌연변이 단백질 SOD1 을 감소시킴으로써 병의 진행을 억제할 수 있을 것이라 생각된다. 또한, 본 연구가 신경퇴행성 질환 이외에도 비정상적인 변성 단백질 축적으로 인해 발생하는 암, 당뇨병, 염증 질환, 심혈관 질환 치료제 개발에 큰 기여를 할 것으로 기대된다.

주요어: 자가포식, 저분자 화합물, 루게릭 병, 퇴행성 뇌 질환, 표현형 기반 스크리닝, 고효율 이미지 기반 스크리닝 시스템, Seoul-Flour 44, 지방 방울, 구조-활성 상관관계, SOD1, 루게릭 병의 *in vitro* 세포 모델

학번: 2011-23231